Materials Research Letters

ISSN: (Print) (Online) Journal homepage: www.tandfonline.com/journals/tmrl20

Ultrahard and super-stable pure aluminum with Schwarz crystal structure

Ling Fang, Yiming Zhong, Bing Wang, Wei Xu, Xiuyan Li & K. Lu

To cite this article: Ling Fang, Yiming Zhong, Bing Wang, Wei Xu, Xiuyan Li & K. Lu (2023) Ultrahard and super-stable pure aluminum with Schwarz crystal structure, Materials Research Letters, 11:8, 662-669, DOI: 10.1080/21663831.2023.2213729

To link to this article: https://doi.org/10.1080/21663831.2023.2213729

MATER. RES. LETT.
2023, VOL. 11, NO. 8, 662–669
https://doi.org/10.1080/21663831.2023.2213729

MATERIALS RESEARCH LETTERS
Taylor & Francis
Taylor & Francis Group

ORIGINAL REPORTS

Ultrahard and super-stable pure aluminum with Schwarz crystal structure

Ling Fang[a,b*], Yiming Zhong[a,b*], Bing Wang[a], Wei Xu[a], Xiuyan Li[a] and K. Lu[a]

[a]Shenyang National Laboratory for Materials Science, Chinese Academy of Sciences, Institute of Metal Research, Shenyang, People's Republic of China; [b]School of Materials Science and Engineering, University of Science and Technology of China, Shenyang, People's Republic of China

ABSTRACT

Refining grains to sub-10 nm size is extremely difficult in pure aluminum due to its high stacking fault energy and low melting point. Herein, we experimentally demonstrate that Schwarz crystal (SC) structure with minimal interfaces constrained by coherent twin boundaries was induced in extremely fine grains (6 nm) of pure aluminum (99.995%) under extremely high shear strain via cryogenic high-pressure torsion. The SC structure exhibits an unprecedented hardness of 2.51 GPa and keeps stable up to 928 K (about 0.99 T_m).

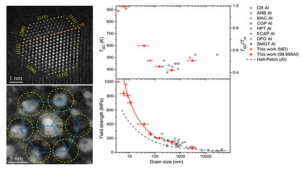

IMPACT STATEMENT

Ultrahard and ultrastable pure aluminum with Schwarz crystal structure has been produced in extremely fine grains under extremely high shear strain via cryogenic high-pressure torsion.

ARTICLE HISTORY
Received 6 April 2023

KEYWORDS
Pure aluminum; Schwarz crystal structure; thermal stability; grain refinement

1. Introduction

Metals can be generally strengthened by controlling the generation of grain boundaries (GBs) that resist dislocation motion. However, extensive experimental results demonstrated that the strengthening effect with decreasing grain size would eventually halt at a critical grain size, below which significant strain softening behavior commences [1–3]. The breakdown of Hall–Petch scaling at the nano scale arises from the enhanced GB instability governed by GB-mediated process, such as GB sliding [3,4] or GB migration [3,5]. The elevated GB instability also makes the nano-sized grains in Al thermally unstable with a much high tendency to coarsen at lower temperature [6–8], making it challenging to apply at elevated temperatures. For these reasons, GBs with high stability are indispensable and favorably expected to achieve high strength in pure Al with nanosized grains.

Recent studies show that nanograins can be stabilized by an autonomous structural evolution to low-energy states, namely GB relaxation, due to the activation of partial dislocation in face-centered-cubic (FCC) metallic materials such as Cu, Ni and Ag as grain sizes are refined to tens of nanometers by cryogenic plastic deformation [9,10]. This discovery sheds light on fabricating more stable nanostructured metals. With the continuous refinement in grain size below 10 nm as well as progressive GB relaxation, Schwarz crystal (SC) structure with minimal interfaces constrained by coherent twin boundaries were discovered in pure Cu [11] and Al–Mg alloy [12] with medium stacking fault energy. This structure is very stable against grain coarsening even at temperature close to the equilibrium melting point, and it can also effectively suppress atomic diffusion.

However, obtaining SC structure in Al is challenging. On one hand, the low melting point of pure Al results in consequently low recovery and recrystallization temperature. This indicates that GBs in the deformed structure are vulnerable against migration under thermal or mechanical stimuli. Besides, the low activation energies for dislocation annihilation promote the

CONTACT Wei Xu wxu@imr.ac.cn Shenyang National Laboratory for Materials Science, Chinese Academy of Sciences, Institute of Metal Research, Shenyang 110016, People's Republic of China
Ling Fang and Yiming Zhong contributed equally to this work.

Supplemental data for this article can be accessed here. https://doi.org/10.1080/21663831.2023.2213729

recovery process, resulting in insufficient dislocation density for dislocation-assisted grain refinement [13,14]. On the other hand, the high stacking fault energy of pure Al makes the formation of twin boundaries harder through conventional plastic deformation, which further hinders the formation of SC structure as a considerable amount of twin boundaries is of necessity in the SC structure to interlock with GB networks.

Lowering deformation temperature may elevate stored dislocation density through suppressing dislocation annihilation and suppressing GB migration. In this way, significant grain refinement in pure Al has been accomplished [8,13]. The commonly observed deformation twinning in pure Al took place for extremely small grains under high enough shear stress [15–17]. However, high pressure promotes the emission of partial dislocations and can increase stacking fault width, leading to a higher propensity of twinning in metals with similar grain size [8,11,18]. For example, we have reported earlier that GB relaxation and twining can be activated in equiaxial nanograined Al with an average grain size of 65 nm processed by cryogenic high-pressure deformation [8]. Then, it is supposed that SC structure can be also induced in pure Al.

In this work, we experimentally demonstrate an SC structure with the grain size of 6 nm in pure Al formed under extremely high shear strain (>50) via cryogenic high-pressure torsion (HPT). The resulted SC structure of Al exhibits an ultrahigh hardness of 2.51 GPa and superior thermal stability (up to 928 K) close to the equilibrium melting point.

2. Experimental

Polycrystalline Al with a purity of 99.995% was annealed at 573 K for 1 h to obtain a fully recrystallized structure with roughly equiaxed grains and then submitted to high-pressure torsion (HPT) processing. HPT was applied to liquid nitrogen using the same procedure as described in the earlier studies [11,12]. Specifically, the samples in the form of discs were deformed on a rectangular flat die with a rotation speed of 30 rpm under a pressure of 10 GPa for different revolutions. The true shear strain is given by [19]

$$\varepsilon = ln\,[1 + (\frac{\theta \times r}{h})^2]^{1/2} + ln\,\frac{h_0}{h}$$

where r is the radius of the disk, θ is the rotation angle, h_0 and h are the initial and final thicknesses, respectively.

The thermal stability of the as-prepared Al samples was determined using isothermal annealing. The samples were sealed in vacuum tubes to prevent possible oxidation during annealing. Annealing of the sealed samples was performed in a vacuum furnace with a protective argon atmosphere and a temperature control accuracy of ±2 K at 373–933 K for 1 h with a ramping rate of 100 K/min. The Vickers hardness (Hv) was measured on a Qness Q10 A + automatic hardness tester with a load of 10 g and a dwell time of 10 s. Each hardness value was obtained by averaging over 10 measurements, and the error bar is the mean standard deviation. Structural characterization was carried out using TEM to provide information on morphology and grain size. Bright-field images and selected area electron diffraction (SAED) patterns were obtained on an FEI Talos F200 TEM operating at 200 kV. Atomic-resolution high-angle annular dark field (HAADF) STEM observations were performed on an aberration-corrected environmental TEM, FEI Titan3 G2 60–300 ChemiSTEM, operated at 300 kV. Electron back-scattered diffraction (EBSD) analysis was carried out on an FEI Nova 430 SEM under a voltage of 20 kV and a current of 6 nA.

3. Results and discussion

3.1. Formation of Schwarz crystal structure in Al

After deformed to a strain of about 5, the microstructure is characterized by roughly equiaxed ultrafine grains with an average grain size of 460 nm (sample UFG-460, Figure S1a-b). Statistical analysis of the GBs reveals the majority of the boundaries are of high angle ones (about 80%, Figure S1c).

As the shear strain increases up to about 23, the grain sizes are in the nanoscale regime, with an average value of ~38 nm (sample NG-38, Figure S1d–e). In contrast to the ultrafine grains, deformation twins were frequently observed at the interior of nano-sized grains as shown in the atomic resolution HAADF-STEM micrograph in Figure S1f. This feature is similar to previous observations in nanograined Al with a grain size of 50–100 nm [8,15], which can be attributed to the large shear strain and low deformation temperature as well as grain size effect [15,17,20,21]. Both molecular dynamics (MD) simulations [20,22] and experimental results [8,10] suggested that full dislocation-mediated deformation may shift to partial dislocation or deformation twinning for some FCC metals when the grain size decreases to tens of nanometers. The emitted partial dislocations would interact with the boundary at the opposite side, giving rise to the dissociation of the original GBs and the relaxation of the GB structure into an ordered morphology with low excess energy. Thus the formation of a considerable amount of twin boundaries in the nanograined Al implies that GBs are relaxed into low-energy states [8,10,23].

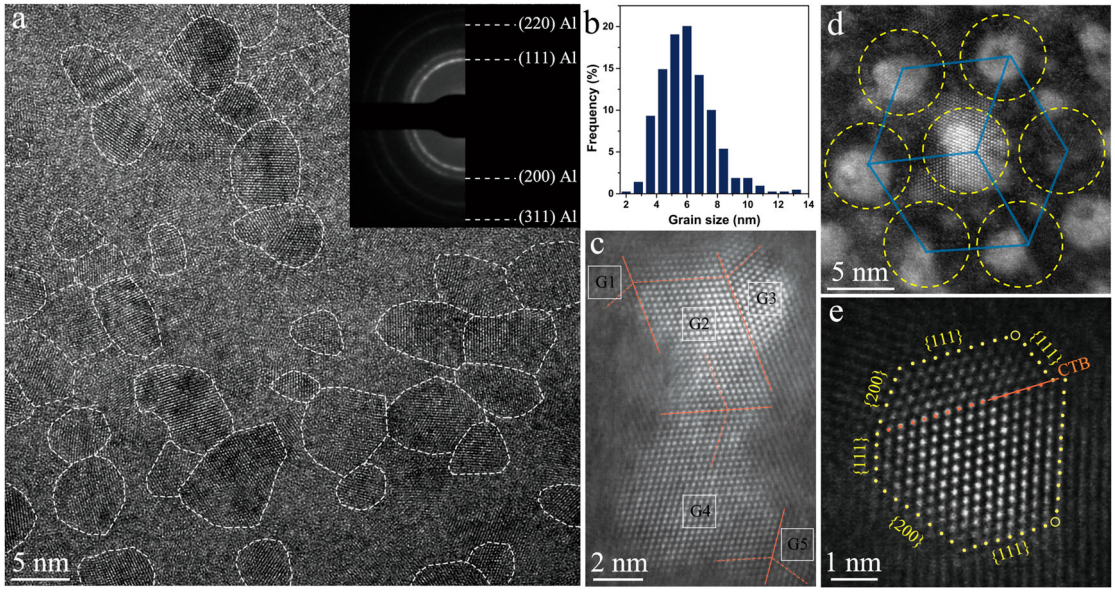

Figure 1. Microstructural characterization of the as-prepared SC-6 sample. (a) Representative high-resolution TEM image showing individual nanograins outlined by dashed white lines and corresponding SAED pattern (inserted). (b) Grain size distribution of the as-prepared sample. (c) A typical high-resolution HADDF-STEM image of the Schwarz crystal containing five grains. Orange dashed lines represent {111} planes and orange solid lines show coherent twin boundaries (CTBs). (d) Atomic resolution HAADF-STEM *D*-SC morphology. (e) Atomic resolution HAADF-STEM image of a tiny grain with a CTB with the beam direction along the [110] zone axis. Missing atoms at several corners are indicated by yellow circles.

At the large strain above 50, extremely fine equiaxed grains with random orientations are observed (Figure 1a). Selected area electron diffraction (SAED) pattern, inserted in Figure 1(a), confirms that the SC-6 sample is a fully nanocrystalline FCC Al. The grain size shows a narrow distribution ranging from 2 to 15 nm, averagely 6 nm (sample SC-6, Figure 1b). By increasing the magnification, irregularly shaped aggregates that consisted of several individual grains of a few nanometers in size are also observed among which twin relationships were frequently identified (Figure 1c). Along the [110] axis, we found there were about 40% nano-sized grains containing one or more through-grain twins with fully coherent {111} twin boundaries in the SC-6 sample. Symbolic honeycombed grains with circular contour are also observed (Figure 1d), which is a typical symmetry character of the SC structure [24]. Magnified HAADF-STEM image indicates that some individual grains exhibited truncated octahedron geometries with many faceted boundary planes at the atomic level (Figure 1e), such as {111} and {100} atomic planes, atomic images at several corners were missing. Statistical analysis of the faceted boundaries revealed that the numbers of {111} and {100} boundary are 60% and 32%, respectively, similar to that in the SC structure Cu and Al–Mg samples with comparable grain size [11,12]. These results suggest that the formation of SC structure can be achieved in purity Al using the cryogenic high-pressure deformation with shear strain of more than 50.

Formation mechanisms of the SC structure in pure Al are the result of deformation-induced GB relaxation into low energy states under cryogenic HPT at extreme shear strain and high imposed hydrostatic stress as grain sizes are refined to tens of nanometers since the deformation mechanism changes from full dislocation to stacking fault or twinning [10], which agrees well with the experimental observations in the present samples (Figure S1f). Larger plastic strain leads to further grain refinement and advancing GB relaxation. With the proceeding of the GB relaxation, more and more faceted {111} and {100} interfaces with low energy would form at the expense of other interfaces to reduce system-free energy. And the grains accordingly show truncated-octahedral shape that is bounded by these low-index atomic planes (Figure 1e). As to the corners and edges of truncated octahedron grains with high surface energy and therefore thermodynamically unstable, they would eventually disappear as subsequent GB reactions (such as dissociation) may be preferentially triggered at these sites. Eventually, the initial whole GB network evolves into the minimal interfaces that are constrained by twin boundaries (Schwarz structure, Figure 1).

3.2. Continuous hardening and strengthening

The deformed Al exhibits a continuous increase in hardness as a function of shear strain (Figure S2). Ultra-high

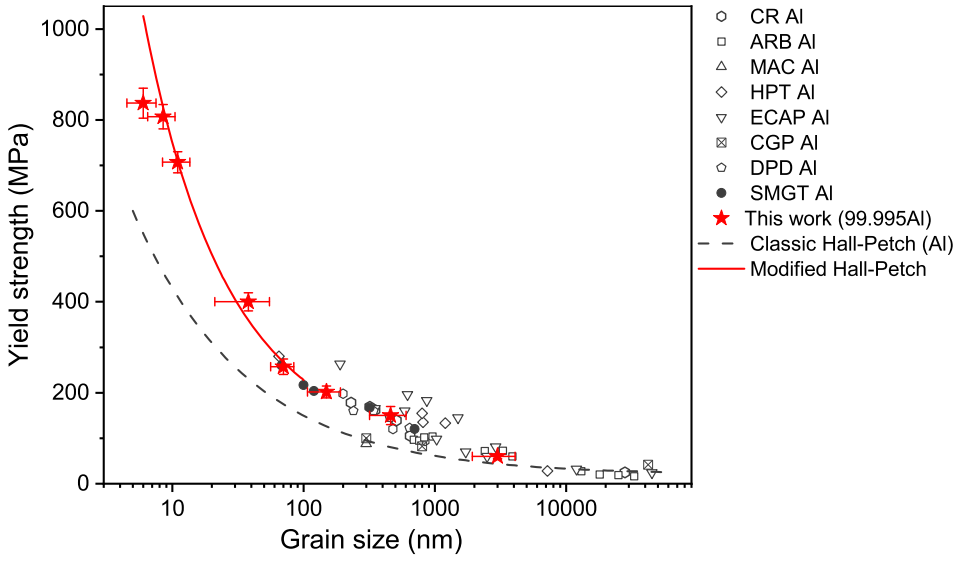

Figure 2. Yield strength (Hv/3) as a function of initial average grain size in pure Al. Literatures data [6,13,25,26,30–40] are included for pure Al with purity above 99.5 processed via various plastic deformation techniques including cold rolling (CR), accumulative roll-bonding (ARB), multi-axil compression (MAC), high-pressure torsion (HPT), equal channel angle pressing (ECAP), constrained groove pressing (CGP), dynamic plastic deformation (DPD) and surface mechanical grinding treatment (SMGT). The gray dash line is a Hall–Petch plot for pure Al.

hardness of 2.51 GPa was obtained in the SC structure Al after cryogenic HPT processing. This hardness value is about 12.5 times that of coarse-grained counterpart, and much higher than reported data on nanostructured Al samples created by severe plastic deformation [8,13,25,26] or gas deposition [27].

Previous studies [2,28] have suggested that size softening would occur as a result of the transition from dislocation-mediated to GB-mediated mechanisms when the grain size or twin thickness is below a critical value of about 10–15 nm in Cu. However, we did not find size-softening behavior in the present study, suggesting that GB-mediated mechanism was significantly suppressed by the relaxed GBs with high stability (Figure S1d–f and Figure 1). As illustrated in Figure 2, the yield strength continuously increases with decreases of d down to sub-10 nm, reaching a value of about 837 MPa at $d = 6$ nm, which follows the principle of 'smaller is stronger'. In addition, the grain size strengthening of nanograined Al is even more pronounced in smaller size range, especially for the grain size refined below 20 nm, largely deviating from the extrapolated Hall-Petch model. Recent experimental work [29] indicates that full-dislocation-mediated deformation mechanisms would shift to both full and partial dislocations in fine nanograins under high pressure. Therefore, we use a modified Hall–Petch relationship as follows [29]:

$$\sigma_y = \sigma_0 + k_0 d^{-1/2} + k_1 d^{-1}$$

where σ_y is the yield strength (taking σ_y = Hv/3), σ_0 is the so-called friction stress in pure Al. k_0 *and* k_1 are constants. The second term represents the classic Hall–Petch low associated with the full dislocation activities. The third term comes from the partial dislocation contribution to yielding, which is proportional to $1/d$. This fit gives a k_0 of 50 MPa $\mu m^{1/2}$ and k_1 of 2 MPa μm, respectively. The fitting of experimental date with the above equation shows that the modified Hall–Petch model can well describe the size strengthening of metallic materials over a wide grain size range.

The coupling effect of partial and full dislocations provides a stronger strengthening route than the classic Hall–Petch relationship and thus lead to a prominent increment in hardness, especially when the grain size has significantly refined into sub-10 nm in the current work with the aid of deformation induced GB relaxation. Besides, prevailed partial dislocation activity in extremely fine nanograins would greatly amplifying the strengthening effect of partial dislocations. A similar enhanced strengthening effect at grain sizes smaller than 20 nm was achieved in nanograined Ni through both partial and full dislocation hardening plus suppression of GB-mediated processes during high-pressure deformation [29]. Therefore, the enhanced Hall–Petch strengthening originates from the excellent mechanical stability of relaxed GBs with suppressed GB sliding and migration as well as increased the critical stresses for nucleating both full and partial dislocations [11,29].

3.3. Excellent thermal stability of the Schwarz crystal structure

Thermal stability of the as-prepared Al samples was determined by isothermal annealing at various temperatures for 1 hour. The change in average grain size and room temperature hardness with annealing temperature is shown in Figure 3(a). As expected, for the UFG-460 sample, apparent grain coarsening with softening occurs at temperature as low as 393 K. With increasing annealing temperature to 423 K, the grain size apparently increased to a few micrometers (Figure S3), which is in accordance with those previously reported [8,34]. In contrast, the NG-38 sample is remarkably thermally stable owing to the mechanical GB relaxation during the cryogenic HPT process [8,10]. There is no obvious change in the size of the grain structures below 600 K (Figure S4), so does the hardness, and the grain coarsening temperature is much higher than the recrystallization temperature of deformed coarse-grained Al(~473 K) [6,8]. The grain size grew rapidly as the annealing temperature exceeded 623 K. Interestingly, grain sizes in the SC-6 sample remained stable after annealing in the same temperature ranges. The average grain size only increased from 6 to 8 nm after annealing at 823 K for 1 h, corresponding to a minor drop in hardness from 2.51 to 2.2 GPa. We further increase the annealing temperature up to 928 K, which is only 5 K below the equilibrium melting of Al of 933 K, the resultant average grain size is about 9.2 nm (Figure 3b and c), SAED pattern (insert in Figure 3b) shows a continuous and random orientation among the Al nanograins, which is very close to that of the as-prepared sample. In addition, we still observed the tiny truncated octahedron-shaped grains and irregularly shaped aggregates constrained by coherent twin boundaries (Figure 3d and e), similar to what we observed before annealing. This result implies that the SC structure does not change after the high temperature treatment.

Plotting grain size and grain coarsening temperature (T_{GC}) data for pure Al with various plastic deformation routes reported in the available literature shows a general tradeoff trend that the smaller the grain size, the lower the instability temperature (Figure 4). The submicro-grained and coarse-grained Al samples fall into the tradeoff region. However, the nanograined samples with grain size below ~65 nm exhibit distinct stability. Smaller nanograins become more thermally stable, and the coarsening temperature of SC structure rises up to 928 K of about 0.99 T_m. It is higher than the recrystallization temperature of deformed coarse-grained Al and Al alloys.

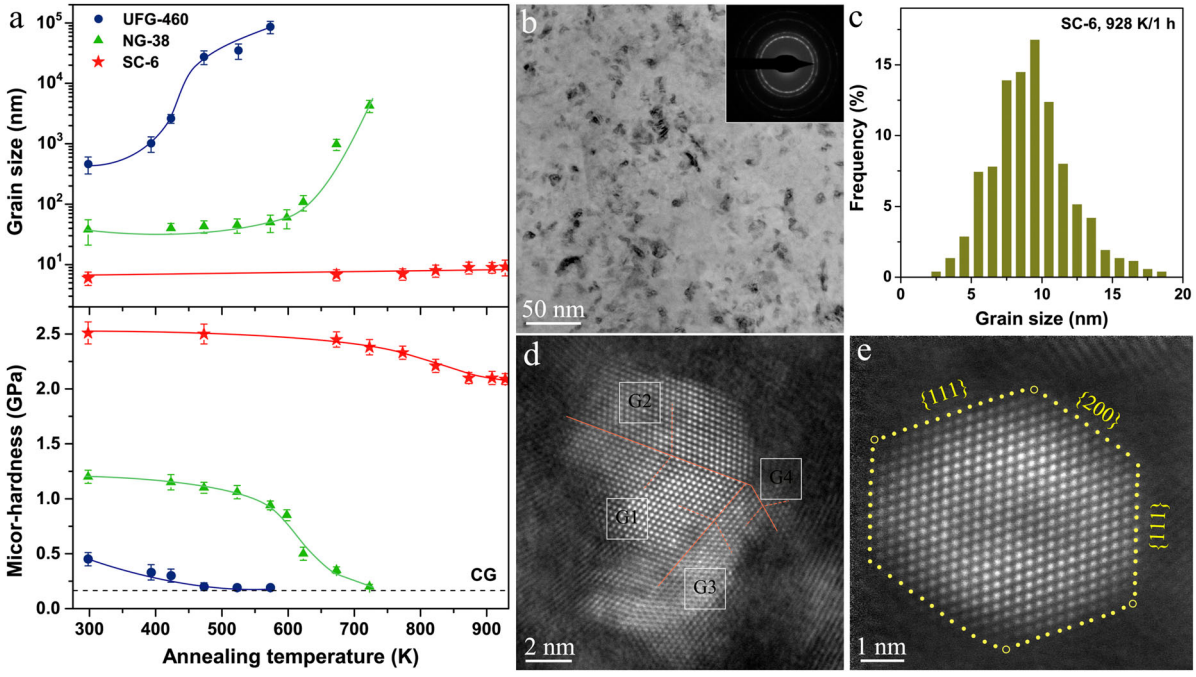

Figure 3. Thermal stability of micro-hardness and grain size. (a) Grain size and micro-hardness variations as a function of annealing temperature (with a duration of 1 h) for three samples with initial average grain sizes of 460, 38, and 6 nm, respectively. Microstructural characterization of the as-annealed SC-6 sample. (b) Bright-field TEM image. (c) The grain size distribution. (d) A typical high-resolution HAADF-STEM image of the Schwarz crystal containing four grains. Orange dashed lines represent {111} planes and orange solid lines show coherent CTBs. (e) Atomic resolution HAADF-STEM image of a tiny grain with a twin-free grain with the beam direction along the [110] zone axis. Missing atoms at several corners are indicated by yellow circles.

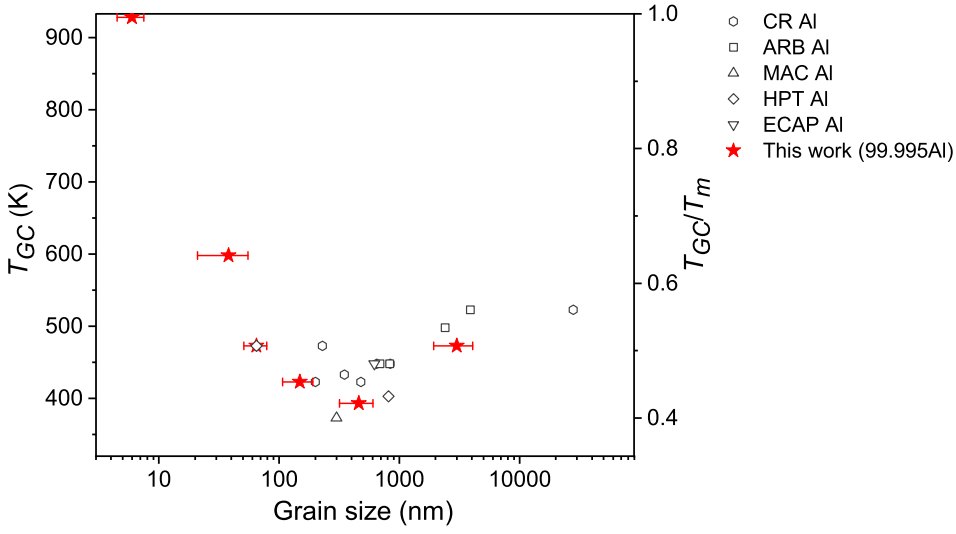

Figure 4. Ultrahigh thermal stability. Grain coarsening temperature (T_{GC}) as a function of initial average grain size in pure Al. Literatures data [6,30,34–36,38–40] are included for pure Al with purity above 99.5 processed via various plastic deformation techniques including cold rolling (CR), accumulative roll-bonding (ARB), multi-axil compression (MAC), high-pressure torsion (HPT) and equal channel angle pressing (ECAP).

According to the kinetic theory of grain growth, the GB migration velocity (v) depends on the GB mobility (M) and the driving force for boundary migration (P), their relationship is described as [41]: $v = MP = M_0 exp(-Q_m/RT)\ C\gamma/r$, where M_0 is the pre-exponential factor, Q_m is the activation energy of GB migration, R is gas constant, T is temperature, C is a constant, γ is the excess energy of GB and r is the radius of curvature, which is generally proportional to the grain size. Based on this model, the GB mobility would be very high as the grain size is reduced to the nanoscale. GB migration velocity can be decreased with the reduction of GB energy. Thus introducing low-energy GBs in pure metals is an effective way to decrease the grain growth rate at elevated temperature. Based on the above model, for the as-prepared Al with grain sizes around tens of nanometers in this work, HAADF-STEM observations revealed that an autonomous structural evolution in GBs toward low energy states by plastic deformation (Figure S1f). The mobility of these low-energy configuration can be significantly reduced, eventually inducing the observed high stability (Figure 4).

The excellent thermal stability of SC structure in Al originates from its minimal-interface area and zero mean curvature remarkably suppressing GB migration at high temperatures since the rate of GB migration is proportional to its curvature [11,41]. In addition, twin boundaries are intrinsically stable even at elevated temperatures. The stability of Schwarz interfaces is further enhanced as they are constrained by twin boundaries (Figure 1).

4. Conclusion

In summary, this work demonstrates that SC structure can be induced in extremely fine grains (6 nm) for pure Al with high stacking fault energy, by applying a very high shear strain over 50 in liquid nitrogen. The SC structure exhibits an ultra-high hardness of 2.51 GPa and superior thermal stability with the coarsening temperature being close to the equilibrium melting point, exceptionally higher than those of conventional pure Al.

Disclosure statement

No potential conflict of interest was reported by the author(s).

Funding

This work was financially supported by the National Natural Science Foundation of China (grant number 52101161 and 52225102), the Young Elite Scientists Sponsorship Program by CAST (grant number 2022QNRC001), the Postdoctoral Science Foundation of China (grant number 2021M693228) and the Ministry of Science and Technology of the People's Republic of China (grant number 2017YFA0700700).

References

[1] Schuh CA, Nieh TG, Iwasaki H. The effect of solid solution W additions on the mechanical properties of nanocrystalline Ni. Acta Mater. 2003;51(2):431–443.
[2] Lu L, Chen X, Huang X, et al. Revealing the maximum strength in nanotwinned copper. Science. 2009;323(5914):607–610.

[3] Schiotz J, Jacobsen KW. A maximum in the strength of nanocrystalline copper. Science. 2003;301(5638):1357–1359.
[4] Chinh NQ, Szommer P, Horita Z, et al. Experimental evidence for grain-boundary sliding in ultrafine-grained aluminum processed by severe plastic deformation. Adv Mater. 2006;18(1):34–39.
[5] Fang TH, Li WL, Tao NR, et al. Revealing extraordinary intrinsic tensile plasticity in gradient nano-grained copper. Science. 2011;331:1587–1590.
[6] Kamikawa N, Huang X, Tsuji N, et al. Strengthening mechanisms in nanostructured high-purity aluminium deformed to high strain and annealed. Acta Mater. 2009;57(14):4198–4208.
[7] Huang XX, Hansen N, Tsuji N. Hardening by annealing and softening by deformation in nanostructured metals. Science. 2006;312(5771):249–251.
[8] Wang B, Xu W, Zhou X, et al. Formation of stable equiaxial nanograined Al via combined plastic deformation. Scr Mater. 2021;203:114054.
[9] Zhou X, Li X, Lu K. Size dependence of grain boundary migration in metals under mechanical loading. Phys Rev Lett. 2019;122(12):126101.
[10] Zhou X, Li X, Lu K. Enhanced thermal stability of nanograined metals below a critical grain size. Science. 2018;360(6388):526–530.
[11] Li XY, Jin ZH, Zhou X, et al. Constrained minimal-interface structures in polycrystalline copper with extremely fine grains. Science. 2020;370:831–836.
[12] Xu W, Zhang B, Li XY, et al. Suppressing atomic diffusion with the Schwarz crystal structure in supersaturated Al–Mg alloys. Science. 2021;373(6555):683–687.
[13] Xu W, Liu XC, Lu K. Strain-induced microstructure refinement in pure Al below 100 nm in size. Acta Mater. 2018;152:138–147.
[14] Sakai T, Belyakov A, Kaibyshev R, et al. Dynamic and post-dynamic recrystallization under hot, cold and severe plastic deformation conditions. Prog Mater Sci. 2014;60:130–207.
[15] Liao XZ, Zhou F, Lavernia EJ, et al. Deformation mechanism in nanocrystalline Al: Partial dislocation slip. App Phys Lett. 2003;83(4):632–634.
[16] Warner DH, Curtin WA, Qu S. Rate dependence of crack-tip processes predicts twinning trends in f.c.c. metals. Nat Mater. 2007;6(11):876–881.
[17] Chen MW, Ma E, Hemker KJ, et al. Deformation twinning in nanocrystalline aluminum. Science. 2003;300(5623):1275–1277.
[18] Cao B, Daphalapurkar NP, Ramesh KT. Ultra-high-strain-rate shearing and deformation twinning in nanocrystalline aluminum. Meccanica. 2014;50(2):561–574.
[19] Zhilyaev AP, McNelley TR, Langdon TG. Evolution of microstructure and microtexture in fcc metals during high-pressure torsion. J Mater Sci. 2006;42(5):1517–1528.
[20] Yamakov V, Wolf D, Phillpot SR, et al. Dislocation processes in the deformation of nanocrystalline aluminium by molecular-dynamics simulation. Nat Mater. 2002;1(1):45–48.
[21] Zhao F, Wang L, Fan D, et al. Macrodeformation twins in single-crystal aluminum. Phys Rev Lett. 2016;116(7):075501.
[22] Rittner J, Seidman DN, Merkle K. Grain-boundary dissociation by the emission of stacking faults. Phys Rev B. 1996;53(8):R4241–R4244.
[23] Xu W, Zhang B, Du K, et al. Thermally stable nanostructured Al-Mg alloy with relaxed grain boundaries. Acta Mater. 2022;226:117640.
[24] Jin ZH, Li X, Lu K. Formation of stable schwarz crystals in polycrystalline copper at the grain size limit. Phys Rev Lett. 2021;127(13):136101.
[25] Yu CY, Kao PW, Chang CP. Transition of tensile deformation behaviors in ultrafine-grained aluminum. Acta Mater. 2005;53(15):4019–4028.
[26] Morattab S, Ranjbar K, Reihanian M. On the mechanical properties and microstructure of commercially pure Al fabricated by semi-constrained groove pressing. Mater Sci Eng A. 2011;528(22–23):6912–6918.
[27] Bufford D, Liu Y, Wang J, et al. In situ nanoindentation study on plasticity and work hardening in aluminium with incoherent twin boundaries. Nat Commun. 2014;5:4864.
[28] Hu J, Shi Y, Sauvage X, et al. Grain boundary stability governs hardening and softening in extremely fine nanograined metals. Science. 2017;355:1292–1296.
[29] Zhou X, Feng Z, Zhu L, et al. High-pressure strengthening in ultrafine-grained metals. Nature. 2020;579(7797):67–72.
[30] Huang T, Shuai L, Wakeel A, et al. Strengthening mechanisms and Hall-Petch stress of ultrafine grained Al–0.3%Cu. Acta Mater. 2018;156:369–378.
[31] Xu C, Horita Z, Langdon TG. The evolution of homogeneity in processing by high-pressure torsion. Acta Mater. 2007;55(1):203–212.
[32] Edalati K, Ito Y, Suehiro K, et al. Softening of high purity aluminum and copper processed by high pressure torsion. Int J Mater Res. 2009;100(12):1668–1673.
[33] Huang F, Tao N. Effects of strain rate and deformation temperature on microstructures and hardness in plastically deformed pure aluminum. J Mater Sci Technol. 2011;27(1):1–7.
[34] Zhao FX, Xu XC, Liu HQ, et al. Effect of annealing treatment on the microstructure and mechanical properties of ultrafine-grained aluminum. Mater Des. 2014;53:262–268.
[35] Bowen JR, Prangnell PB, Juul Jensen D, et al. Microstructural parameters and flow stress in Al–0.13% Mg deformed by ECAE processing. Mater Sci Eng A. 2004;387-389:235–239.
[36] Yu CY, Sun PL, Kao PW, et al. Evolution of microstructure during annealing of a severely deformed aluminum. Mater Sci Eng A. 2004;366(2):310–317.
[37] Shin DH, Park J-J, Kim Y-S, et al. Constrained groove pressing and its application to grain refinement of aluminum. Mater Sci Eng A. 2002;328(1–2):98–103.
[38] Kamikawa N, Hirochi T, Furuhara T. Strengthening mechanisms in ultrafine-grained and sub-grained high-purity aluminum. Metall Mater Trans A. 2019;50(1):234–248.
[39] Sun P-L, Zhao Y, Tseng T-Y, et al. Annealing behaviour of ultrafine-grained aluminium. Philos Mag. 2013;94(5):476–491.

[40] Mavlyutov AM, Latynina TA, Murashkin MY, et al. Effect of annealing on the microstructure and mechanical properties of ultrafine-grained commercially pure Al. Phys Solid State. 2017;59(10):1970–1977.

[41] Porter DA, Easterling KE. Phase transformations in metals and alloys. Revised Reprint, Boca Raton: CRC Press; 2009.